euronoise

On the influence of the micro-geometry on sound propagation through periodic array of cylinders

Rodolfo Venegas and Olga Umnova

University of Salford, Acoustics Research Centre, Newton Building, M5 4WT Salford, UK
r.g.venegascastillo@pgr.salford.ac.uk

Sound propagation in rigid porous media has been widely studied by using semi-phenomenological models. These models make use of a set of averaged macroscopical parameters to represent the microscopic details of the porous media geometry and, in a certain way, their influence on the acoustical properties is not directly identified. In this paper, homogenization theory and finite element method are used for solving the full microscopic dynamic flow and heat transfer problems for a porous medium modelled as an idealized periodic array of cylinders. Different cross-section shapes of the cylinders (circular, ellipsoidal and square) and a wide range of porosity values are considered. The full simulations are compared with standard semi-phenomenological models of sound propagation in porous media. The influence of the micro-geometry on the acoustical quantities such as speed of sound, attenuation coefficient and absorption coefficient is analysed and proved to be significant especially at low porosities.

1 Introduction

Acoustics of porous media is a vastly studied subject which requires the knowledge of different branches of physics. The main areas involved in the acoustic characterization of a porous material are fluid dynamics and heat transfer theory. Different approaches to characterizing porous materials have been suggested during the past decades which mainly fall into three major categories, i.e. empirical models, semi-phenomenological models and direct simulations based on a microstructural approach. Empirical models, as the name suggests, are based on fitting experimental data and proposing empirical laws [1]. The main drawback of this approach is given by the non-general nature of the proposed fitted functions and the range of applicability limited to the physical characteristics of the materials measured. Semi-phenomenological models are based on proposing scaling functions, which depend on macroscopical independently measurable parameters to describe viscous and thermal behaviour of the medium. Within this category, one of the most important contributions has been made by Johnson et al. [2], who introduced the concept of dynamic tortuosity to describe frequency-dependent viscous interactions between the pore fluid and the frame. It depends on dc viscous permeability, porosity, tortuosity and viscous characteristic length, all of which can be independently measured. The complete acoustic characterization however should also consider the thermal behaviour of the porous medium. The work by Champoux and Allard [3] further complemented by Lafarge et al. [4] serves this purpose. They introduced another scaling function, complex compressibility, which depends on dc thermal permeability, porosity and thermal characteristic length. The combined Jonhson-Champoux-Allard-Lafarge model (called JCAL henceforth) is now widely accepted. However, it is not sufficiently accurate in the frequency range where both viscous and inertial interactions are important [5,6], especially when dealing with more extreme geometries like very pronounced variable-width channels [5]. The behaviour of JCAL model was corrected by Pride et al. [5] by introducing two additional parameters, the so-called low-frequency viscous and thermal tortuosities, thus ending up with a total of eight parameters needed to fully describe the acoustic properties of a rigid porous material. This model will be referred to as Pride-Johnson-Champoux-Allard-Lafarge (PJCAL) model in this work from now on. The main drawback of this approach is the difficulty in measuring all the parameters involved in the modelling.

The approach to be used in this work corresponds to the direct numerical simulation based on homogenization theory [7,8]. This theory provides a rigorous method of deducing empirical laws, such as for example the dynamic Darcy's law [8]. Homogenization theory gives the governing equations at different levels. The main hypothesis behind this theory is the separation of scales, which in the context of porous media acoustics, is usually valid when sound wavelength exceeds the characteristic size of the medium. The equations at the respective level are solved in a representative elementary volume (REV) of the porous medium geometry by using an appropriate analytical or numerical method. The main drawback of this approach is the computational time and the use of relatively simplistic inner structure to represent the porous medium. Nevertheless, with the advent of powerful desktop machines this problem seems to be less relevant nowadays.

In this paper a numerical study of the influence of the micro-geometry on dynamic tortuosity, dynamic bulk modulus and acoustical quantities such as sound propagation, attenuation coefficient and absorption coefficient is presented. The geometries under consideration, i.e. periodic arrays of cylinders with different cross-section shapes, provide an idealized representation of a fibrous material. The finite element method is used for the solution of the full microscopic dynamic flow and heat transfer problems as well as for calculation of the semi-phenomenological (JCAL and PJCAL) models parameters. The paper is organized as follows. In section 2 the relevant expressions for the acoustical quantities and the governing equations to be solved are introduced. Results and discussions are presented in section 3. Conclusions correspond to the last section of this work.

2 Theory and Methods

It is assumed that the medium under study is homogenous, isotropic and having a rigid porous. The porous solid with porosity ϕ is saturated by a Newtonian fluid of density ρ_0 and viscosity η. The wavelength of sound λ is assumed to be much larger than any characteristic pore or inclusion size. The linear response of a medium to an oscillatory, with angular frequency ω, macroscopic gradient of pressure, $\nabla p_e e^{j\omega t}$, is related to the spatial average ($\langle\cdot\rangle = \int_{\Omega_f} \cdot d\Omega / |\Omega|$) of the fluid velocity $u(\omega)$ over the fluid phase Ω_f in a REV (Ω) by mean of the dynamic extension of the Darcy's law [2,8].

$$\langle u(\omega) \rangle = -K(\omega)\nabla p_e / \eta . \quad (1)$$

The viscous interactions between the frame and the fluid are determined through the complex frequency-dependent dynamic density function $\rho(\omega)$, which is related to dynamic permeability $K(\omega)$ and dynamic tortuosity $\alpha(\omega)$ as follows :

$$\rho(\omega) = \alpha(\omega)\rho_0 = \eta\phi / j\omega K(\omega) . \quad (2)$$

Fluid velocity is calculated from the solution of an oscillatory forced Stokes flow problem. At the microscopic level, as the homogenization theory states, this is described by the following governing equations [8]:

$$\begin{aligned} &\eta\nabla^2 u - \nabla p - \nabla p_e - ju\omega\rho_0 = 0 \ \text{ in } \Omega_f , \\ &\nabla \cdot u = 0 \ \text{ in } \Omega_f \qquad\qquad u = 0 \ \text{ on } \Gamma. \end{aligned} \quad (3)$$

No slip condition on the boundary Γ of the porous solid is applied as well as periodicity conditions on the elemental cell boundary. The latter implies zero total boundary force per unit of area and periodic constrictions upon velocity components and pressure. An arbitrary pressure was prescribed at one of the vertices of the cell in order to specify the pressure and to keep the boundary conditions unchanged [9].

The oscillatory heat transfer between the frame (cylinders in this case) and the fluid is described by the dynamic bulk modulus $K_a(\omega)$, which is calculated from an analogous dynamic thermal Darcy's law [4]:

$$\langle T(\omega) \rangle = j\omega K'(\omega)/\kappa , \quad (4)$$

$$K_a(\omega) = \frac{\gamma P_0}{C(\omega)} = \frac{\gamma P_0}{\left(\gamma - j\omega\rho_0 \dfrac{(\gamma-1)C_p K'(\omega)}{\kappa\phi} \right)} , \quad (5)$$

where κ is thermal conductivity of the fluid, C_p is the specific heat at constant pressure, γ is the adiabatic constant and P_0 is atmospheric pressure.

Dynamic bulk modulus varies from its isothermal value P_0 at low frequencies to the adiabatic value γP_0 at high frequencies. As can be seen from the above, this function is related to the dynamic thermal permeability $K'(\omega)$ and dynamic compressibility $C(\omega)$.

The spatially averaged temperature difference between the fluid and the frame $\langle T(\omega) \rangle$ is calculated from the solution of the following problem:

$$\begin{aligned} &\kappa\nabla^2 T - j\omega\rho_0 C_p T + j\omega p_0 = 0 \ \text{ in } \Omega_f , \\ &T = 0 \ \text{ on } \Gamma. \end{aligned} \quad (6)$$

Thermal insulation condition and periodic boundary conditions for the temperature are set on the boundaries of the cell.

The acoustical behaviour of a porous material is completely determined by the wave number $q(\omega)$ and the characteristic impedance $Z_c(\omega)$, [4], which are related to the dynamic density and dynamic modulus as follows:

$$q(\omega) = \omega\sqrt{\rho(\omega)K_a^{-1}(\omega)} , \quad (7)$$

$$Z_c(\omega) = (1/\phi)\sqrt{\rho(\omega)K_a(\omega)} . \quad (8)$$

If one considers a rigidly terminated layer of porous material, with thickness *d,* the surface impedance can be calculated as:

$$Z_w(\omega) = Z_c \coth(jqd) . \quad (9)$$

For this configuration, the reflection coefficient and absorption coefficient are calculated as follows:

$$R(\omega) = (Z_w - Z_0)/(Z_w + Z_0) , \quad (10)$$

$$\alpha_s = 1 - |R|^2 , \quad (11)$$

here $Z_0 = \rho_0 c_0$ is the characteristic impedance of air, and c_0 is sound speed.

Finally, the speed of sound, $c(\omega)$, in the porous medium and attenuation coefficient, $a_t(\omega)$ are given by:

$$c(\omega) = \omega / \mathrm{Re}\{q(\omega)\} , \quad (12)$$

$$a_t(\omega) = -\mathrm{Im}\{q(\omega)\} . \quad (13)$$

The semi-phenomenological models to be compared with the direct numerical simulations are JCAL [2,3,4] and PJCAL [5]. In these models, the dynamic density and dynamic bulk modulus are defined as follows:

$$\rho_{(J,P)}(\omega) = \rho_0\alpha_\infty \left(1 - j\omega_c^{(v)} F^{(v)}{}_{(J,P)}(\omega)/\omega \right), \quad (14)$$

$$K_{a(J,P)}(\omega) = \gamma P_0 \left(\gamma - (\gamma-1)\left(1 - \frac{j\omega_c^{(t)} F^{(t)}{}_{(J,P)}}{\omega} \right) \right)^{-1} , \quad (15)$$

with the scaling functions given by:

$$F^{(v,t)}{}_J = \sqrt{1 + jM^{(v,t)}\omega_c^{(v,t)}/2\omega} , \quad (16)$$

$$F^{(v,t)}{}_P = 1 - p_{(v,t)} + p_{(v,t)}\sqrt{1 + jM^{(v,t)}\omega_c{}^{(v,t)}/\omega p^2{}_{(v,t)}} . \quad (17)$$

Here subscripts J and P refer to JCAL and PJCAL respectively. The symbols v and t denote viscous- and thermal-related quantities. Dc viscous permeability k_0 is calculated from the solution of equations (3) by setting frequency equal to zero and then by using Eq.(1).

Tortuosity α_∞ and viscous characteristic length Λ are defined as follows [2]:

$$\alpha_\infty = |\Omega_f| \Big/ \int_{\Omega_f} |E|^2 \, d\Omega , \quad (18)$$

$$\Lambda = 2\int_{\Omega_f} |E|^2 \, d\Omega \Big/ \int_\Gamma |E|^2 \, d\Gamma , \quad (19)$$

where $E = e - \nabla u_\infty$, e a unitary force vector in the direction of the applied gradient of pressure and u_∞ is the solution of the limiting oscillatory viscous flow problem for the high-frequency regime:

$$\begin{aligned} &\nabla^2 u_\infty = 0 \qquad \text{in } \Omega_f , \\ &n \cdot \nabla u_\infty = e \cdot n \qquad \text{on } \Gamma, \end{aligned} \quad (20)$$

where n is the normal vector to Γ. As usual, the periodic boundary conditions are assumed on the cell boundaries [2].

Thermal characteristic length Λ' is a geometrical parameter defined as [3]:

$$\Lambda' = 2\int_{\Omega_f} d\Omega \Big/ \int_{\Gamma} d\Gamma \,. \tag{21}$$

Dc thermal permeability k_0' is given as [4]

$$k_0' = \langle T_0 \rangle \,, \tag{22}$$

where T_0 is the solution of the stationary heat transfer problem: $\nabla^2 T_0 + e_s = 0$; e_s is the thermal scalar equivalent of the unit force vector in the flow problem. Boundary conditions for T_0 are the same as for the oscillatory problem given by Eq. (6) [4].

The viscous and the thermal shape factors $M^{(v,t)}$ are given by $8k_0\alpha_\infty / \phi\Lambda^2$ and $8k_0' / \phi\Lambda'^2$ respectively. The viscous characteristic frequency, $\omega_c^{(v)} = \eta\phi / \alpha_\infty k_0 \rho_0$, indicates the transition from the viscous regime at low frequencies to the inertial one at high frequencies. In a similar way, the thermal characteristic frequency, $\omega_c^{(t)} = \kappa\phi / \alpha_\infty k_0' C_p \rho_0$, denotes the transition from isothermal propagation to the adiabatic one.

The additional parameters in the PJCAL model are $p_{(v)} = M^{(v)} / 4(\alpha_0 / \alpha_\infty - 1)$ and $p_{(t)} = M^{(t)} / 4(\alpha_0' - 1)$, where the low-frequency tortuosity α_0 and its thermal equivalent α_0' are defined as follows [5,6]:

$$\alpha_0 = \left\langle |u_0|^2 \right\rangle / \left| \langle u_0 \rangle \right|^2 , \tag{23}$$

$$\alpha_0' = \left\langle T_0^2 \right\rangle / \langle T_0 \rangle^2 \,. \tag{24}$$

The finite element method was employed for solving all the equations presented in this section. For the flow problem a second-order lagrangian elements model the velocity components and linear ones model the pressure. Second-order lagrangian elements were used for temperature in the thermal problem. The finite element analysis software Comsol Multiphysics [9] was used. It is worth noting that the physical parameters used in JCAL and PJCAL models have directly been calculated from their definitions.

3 Results and Discussion

Regular periodic array of circular (PACC), square (PASC) and ellipsoidal (PAEC) cylinders have been studied. In every case, the half-length of the square cell l (equal to 1 mm in every simulation) was set as a function of the radius r of the circular cylinders in PACC and porosity: $l = r\sqrt{\pi / (1-\phi)}$ .The length side a of the square cylinders in PASC was set equal to $a = r\sqrt{\pi}$. The ellipsoidal cylinders with semi-major axes $h = r\sqrt{2}$ and semi-minor axes equal to $h/2$ have been chosen to form PAEC array. As every configuration had the same inclusion area for a given porosity, the direct study of the shape influence on acoustical quantities has been made possible. Simulations were performed in the frequency range 0-5000 Hz and for porosity values in the range $[0.6, 0.99]$ for PACC and PASC, and $[0.66, 0.99]$ for PAEC due to close packing constrictions. Rotation of the cylinders in PAEC (0° to 90°, steps of 15°) and PASC (0° to 45°, steps of 15° due to symmetry) has also been investigated.

In this paper, only those results which correspond to *porosity value of 0.8* are shown. The reader is encouraged to read the additional material for other porosities [10].

Some of the configurations studied as well as corresponding static fluid flow fields are shown in figure 1 for PACC, PASC rotated by 0° and 45° (PASC0 and PASC45; top, right to left) and PAEC rotated by 0°, 45°and 90° (PAEC0, PAEC45 and PAEC90; bottom, right to left). The harmonic pressure gradient was applied in the vertical direction.

Dynamic tortuosity of every configuration studied is shown in figure 2. There are remarkable differences among dynamic tortuosity functions for different geometries, with PAEC0 (red line) and PAEC90 (brown line) being the most extreme cases for both real and imaginary parts. The differences for both real and imaginary parts increase as the separation between the cylinders decreases. Physically, this means that viscous friction is more prominent in the narrow parts of the channels.

As shown in figure 3, the dynamic bulk modulus (presented normalized to its isothermal value) is less sensitive to the shape of the cylinders even in the case of lower porosities [10]. Moreover, due to the scalar nature of the oscillatory heat transfer problem, this function shows a symmetric behaviour for the periodic array of ellipses with PAEC45 being the symmetry axis. This means that the pairs (PAEC0, PAEC90), (PAEC15, PAEC75) and (PAEC30, PAEC60) have exactly the same values of dynamic bulk modulus. This suggests that viscous-related functions are more sensitive to the changes in the micro-geometry.

Figure 4 displays the results of direct numerical simulations of speed of sound and attenuation coefficient compared with those predicted by JCAL and PJCAL models. The parameters of the models are presented in the additional material (See Table A.1 in [10]). The influence of the cylinder shape on the acoustical properties of the arrays can be quite strong in the frequency range under consideration. The average relative difference between PAEC0 and PAEC90 is 33.56% in speed of sound and 52.73% in attenuation coefficient. The relative error between the results of full numerical simulations and the model predictions is shown in figure 5. For speed of sound, the relative error is very small with maximum value of 3% for JCAL and 1% for PJCAL. In the case of attenuation coefficient, both JCAL (bottom right) and PJCAL (bottom right) give greater deviations from the results of the full numerical simulations with error in some cases exceeding 10%.

In general, PJCAL shows better agreement with the full numerical simulation results than JCAL model.

For PAEC with porosity equal to that of close packing (0.66), the relative error in sound speed averaged over the whole frequency range can reach values of 1.1% for JCAL and 0.7% for PJCAL. For the attenuation coefficient, the averaged relative error does not show a strict pattern, however it tends to increase proportionally to porosity in the case of JCAL. The same situation occurs when using PJCAL, with only a slight increment in error at higher porosities. For JCAL, the maximum averaged error in attenuation coefficient is around 17% for porosities equal to 0.7 and 0.99. For PJCAL, this maximum is around 14%

when porosity is equal to 0.7. The reason for this apparent coincidence is being investigated.

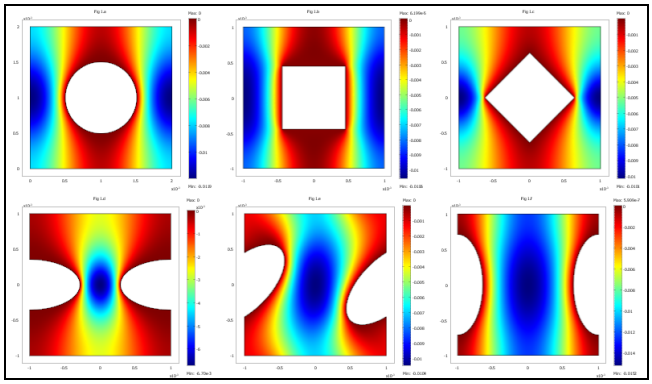

Fig.1 Static fluid velocity, vertical component, $\phi = 0.8$. Top, right to left: PACC, PASC0 and PAC45. Bottom, right to left: PAEC0, PAEC45 and PAEC90

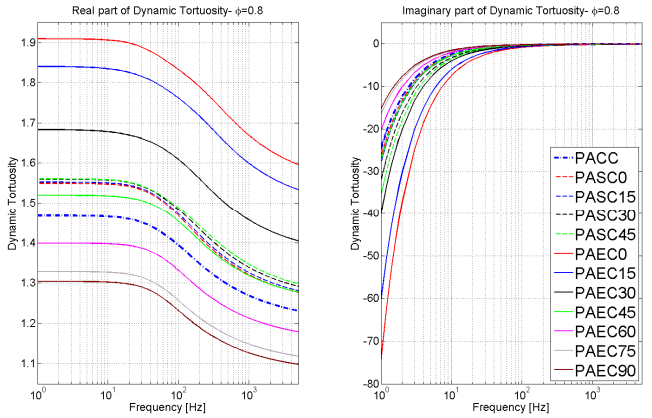

Fig.2 Dynamic tortuosity – full numerical simulation results for different arrays, $\phi = 0.8$.

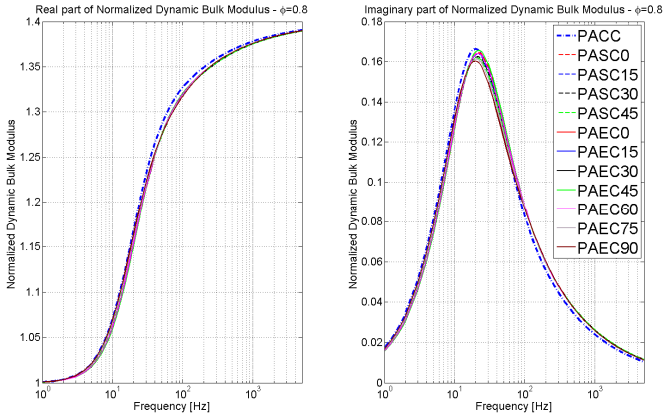

Fig.3 Normalized dynamic bulk modulus - full numerical simulation results for different arrays, $\phi = 0.8$.

Absorption coefficient for a rigidly-backed layer of porous material is presented in figure 6. The thickness of the layer was set equal to d=10 cm. In order to make the figure clearer, only full numerical simulation results are shown.

It is important to note that configurations with the same porosity and thickness give very different results in terms of both amplitude and sound absorption peaks depending on their micro-geometry. As it was pointed out before, PAEC0 (red line) and PAEC90 (brown line) are the most extreme configurations. PAEC0 has, on average over the frequency, 31.2% more sound absorption than PAEC90 and its absorption peaks are shifted to the lower frequency range by around 19.9% on average compared to the ones of PAEC90. This trend is even more pronounced at porosities lower than 0.8 whereas for higher porosities the increment of the absorption tends to be less important as well as the shift in the peaks. This result proves that the shape is much less important for higher porosities and would explain why empirical models, like the model proposed in [1], give reasonably accurate description of sound attenuation by high porosity absorbents.

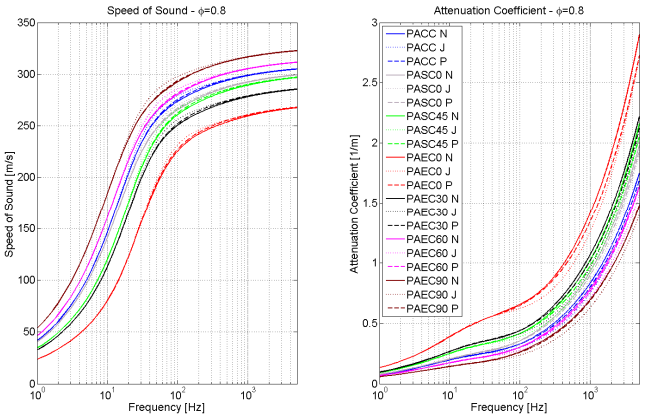

Fig.4 Speed of sound (left) and attenuation coefficient (right) – full numerical simulation results for different arrays (N) and predictions of semi-phenomenological models (J-JCAL, P-PJCAL), $\phi = 0.8$.

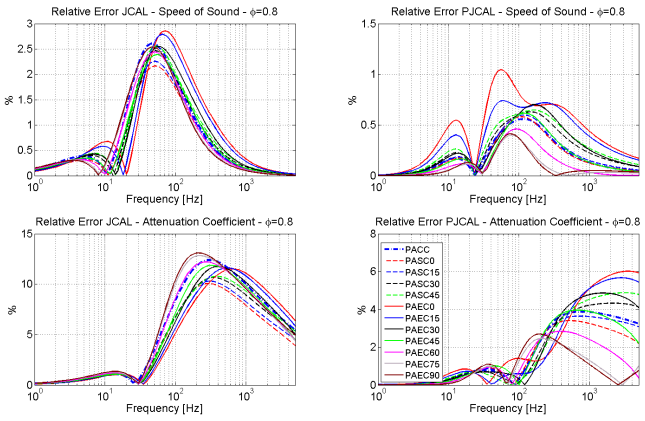

Fig.5 Relative error in speed of sound and attenuation coefficient between full numerical simulations and semi-phenomenological models, $\phi = 0.8$.

The difference in sound absorption of PAEC0 compared to that of PAEC90 is due to the viscous losses inasmuch as their thermal behaviour is identical. This is also the case for PAEC30 and PAEC60 as well as for other symmetrical configurations. Both semi-phenomenological models considered here underestimate sound absorption coefficient. However, PJCAL is still more accurate than JCAL.

In general, if the separation between the cylinders is smaller the viscous losses are greater, therefore sound absorption augments. This fact may explain the similar behaviour of the absorption coefficients for PAEC30 and PASC45 as the

minimum separation between the cylinders is almost the same. These results suggest that the spatial orientation of the cylinders may have a strong influence on acoustical quantities.

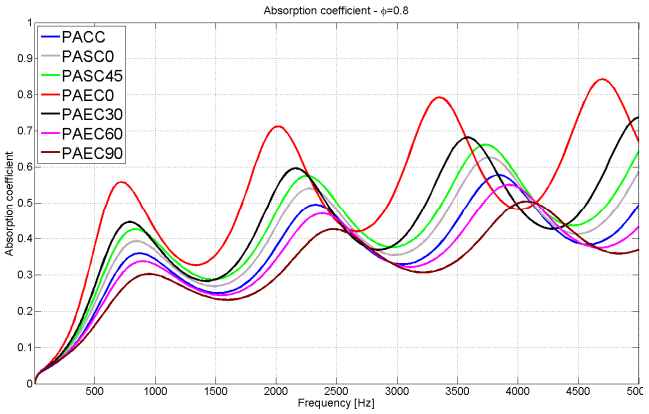

Fig.6 Absorption coefficient, $\phi = 0.8$.

5 Conclusion

The problem of the full numerical simulation of sound propagation in a rigid porous medium modelled as a periodic array of cylinders with different cross-section shapes has been addressed. Full numerical simulation results have been compared with semi-phenomenological model predictions such as JCAL and PJCAL.

It was shown that there is a strong influence of the shape and the orientation of the cylinders on the viscous-related quantities. This influence is weaker for those quantities related to the temperature distribution around the cylinders. The influence is clearly more pronounced at lower porosities whereas at higher porosities the shape and the orientation of the cylinders appear to be less important. This fact would explain why empirical models work well for higher porosity materials.

It is also concluded that speed of sound is less sensitive to the shape of the cylinders than attenuation coefficient and normal incidence absorption coefficient of a layer.

When compared to the numerical results, the PJCAL model shows better performance than JCAL model. However, both models provide a reasonably accurate and fast way of predicting the acoustic properties of the studied idealised structures. This statement is even more appropriate if one considers the computational time required for the full numerical simulations.

The absorption coefficient of a rigidly-backed layer of porous material is shown to be quite sensitive to the changes in cylinder shape and orientation. Amongst the studied arrays, PAEC0 appears to be the most efficient in terms of sound absorption due to its minimum separation between the cylinders. This result is related to the fact that viscous losses are greater in the narrowest parts of flow channels.

The numerical procedure described in this paper is general and can be easily applied to more complex geometries taking special care at lower porosities, where the numerical problem is harder to solve.

Certainly, dynamic tortuosity is calculated from dynamic permeability, which is a second order tensor. In this work some entries of this tensor were calculated only. The complete characterization of the dynamic viscous permeability tensor requires the simulation of the parallel flow problem, which will be addressed in future work.

Acknowledgments

The author gratefully acknowledges an ORSAS award and a University of Salford research studentship.

References

[1] Delany, M. E. and E. N. Bazley. "Acoustical properties of fibrous absorbent materials", *Applied Acoustics* 3(2): 105-116 (1970).

[2] Johnson, D. L., Koplik, J. and Dashen, R., "Theory of dynamic permeability and tortuosity in fluid-saturated porous media", *J. Fluid Mech.* 176, 379-402. (1987).

[3] Champoux,Y. and Allard, J.F., "Dynamic tortuosity and bulk modulus in air-saturated porous media", *J. Appl. Phys*. 70, 1975-1979 (1991).

[4] Lafarge. D., Lemarinier, P., Allard. J. F. and Tarnow, V., "Dynamic compressibility of air in porous structures at audible frequencies", *J. Acoust. Soc. Am* 102 (4), 1995-2006 (1997).

[5] Pride, S. R., Morgan, F. D. and Gangi, A. F., "Drag forces of porous-medium acoustics", *Phys. Rev. B* 47, 4964-4975 (1993).

[6] Cortis, A., Smeulders, D., Lafarge, D., Firdaouss, M. and Guermond, J. L. "Geometry Effects on Sound in Porous Media". *IUTAM Symposium on Theoretical and Numerical Methods in Continuum Mechanics of Porous Materials*: 187-192 (2002).

[7] Sanchez-Palencia, E., "Nonhomogeneous Media and Vibration theory". *Lect. Notes in Physics,* vol. 127, Springer Verlag, Berlin (1980).

[8] Auriault, J.-L., Borne, L. and Chambon, R., "Dynamics of porous saturated media, checking of the generalized law of Darcy." *J. Acoust. Soc. Am*,77(5): 1641-1650 (1985).

[9] COMSOL Multiphysics 3.3a Documentation, www.comsol.com.

[10] Venegas, R. and Umnova, O., "On the influence of the micro-geometry on sound propagation through periodic array of cylinders". Additional material, *Proc. Acoustics'08*. June 29 – July 4, 2008. Paris, France. Also available at http://rodolfo.venegas.googlepages.com.